THE ASTROPHYSICAL JOURNAL, 563:374–380, 2001 December 10

ON THE CORRELATION BETWEEN CORONAL AND LOWER TRANSITION REGION STRUCTURES AT ARCSECOND SCALES

A. VOURLIDAS
CEOSR/CSI, George Mason University, Fairfax, VA 22030; vourlidas@nrl.navy.mil
J. A. KLIMCHUK AND C. M. KORENDYKE
Space Science Division, Naval Research Laboratory, Washington, DC 20375
T. D. TARBELL
Lockheed Martin Solar and Astrophysics Lab, Palo Alto, CA 94304
AND
B. N. HANDY
Department of Physics, Montana State University–Bozeman, Bozeman, MT 39717
Received 2001 July 24; accepted 2001 August 15

ABSTRACT

We compare the morphology of active region structures observed in the 171 Å ($T \sim 9 \times 10^5$ K) and Lyα ($T \sim 2 \times 10^4$ K) lines. The coronal data were obtained by the *Transition Region and Coronal Explorer* (*TRACE*) in support of the Very High Angular Resolution Ultraviolet Telescope (VAULT) sounding rocket launch, which acquired subarcsecond resolution images of an active region in the Lyα line, on 1999 May 7. Using a pair of calibrated, nearly simultaneous images, we find that: (i) a very good correlation exists between the Lyα and 171 Å intensities in the *TRACE* moss regions, (ii) we can identify several identical structures in some (but not all) moss areas, and (iii) the correlations are greatly reduced at the footpoints of the 171 Å large-scale loops. We derive a lower limit for the Lyα emission measure, under the assumption of effectively optically thin emission, and compare it to the 171 Å emission measure. As in previous studies, we find an excess of Lyα material compared to the amount expected for a thermal conduction-dominated corona-chromosphere transition region, even for structures that appear to be identical in the two wavelengths. This result implies that some other mechanism besides classical heat conduction from the corona must contribute to the observed Lyα intensities. The observations do not support the idea of a physically distinct cool loop component within active regions.

Subject headings: Sun: atmosphere — Sun: corona — Sun: transition region — Sun: UV radiation

The investigation of the physics of the solar atmosphere has been invigorated in the 1990s with the launch of several space-based instruments capable of high spectral and spatial resolution. The center of attention has been the long-standing issue of the coronal heating mechanism(s) and consequently the coupling of the cool 10^4 K chromosphere with the million-degree corona through the transition region. The physical properties of this interface, such as temperature, density, and emission measure, have been extensively studied via EUV and UV spectrometers of ever increasing spatial and spectral resolution. The original view of a conductively heated transition region (e.g., Gabriel 1976) in hydrostatic equilibrium has been challenged by these observations (e.g., Feldman 1983), and it remains unclear to what extent the transition region plasmas responsible for the observed emission are actually coupled to the corona (Feldman & Laming 1994; Wikstøl, Judge, & Hansteen 1998).

Part of the uncertainty in the interpretation of spectral line observations arises from their limited spatial coverage. Images are usually built up through rasters that can take anywhere from a few minutes to hours to complete, thus hindering the study of the dynamical evolution and spatial relation of the plasmas in different temperature regimes. The morphology of the solar atmosphere can be more easily studied with broadband filter telescopes such as the EUV Imaging Telescope (EIT; Delaboudinière et al. 1995) aboard the *Solar and Heliospheric Observatory* (*SOHO*; Domingo, Fleck, & Poland 1995) and the *Transition Region and Coronal Explorer* (*TRACE*; Handy et al. 1999a). The *TRACE* filters, in particular, cover the temperature range from the chromosphere to the corona with arcsecond resolution and provide exciting clues about the structure of the atmosphere. One such result is the observation of low-lying EUV emission above magnetic plage, called "moss" because of its patchy appearance (Schrijver et al. 1999; Berger et al. 1999; Fletcher & De Pontieu 1999; De Pontieu et al. 1999). This emission was first identified in soft X-ray images from the Normal Incidence X-ray Telescope (NIXT; Peres, Reale, & Golub 1994). It is best seen in the *TRACE* 171 Å channel and has been interpreted as the conductively heated upper transition region ($\sim$ 1 MK) interface at the legs of very hot ($\sim$ 3–10 MK), soft X-ray emitting loops (Martens, Kankelborg, & Berger 2000). De Pontieu et al. (1999) analyzed high-resolution observations from the Swedish Vacuum Solar Telescope (SVST; Sharmer et al. 1985) and did not find a good correlation between the EUV moss and the photosphere or lower chromosphere. This result puts into question the classical view of a continuous atmosphere through structures in the plage transition region. De Pontieu et al. (1999) attempted to reconcile the discrepancy by proposing a more complex magnetic topology for the transition region. According to their model, a given coronal loop might originate from the interaction of field lines from several photospheric footpoints (Berger et al 1999, Fig. 6).

An aspect that has not been sufficiently exploited so far is the relation of the upper chromosphere/lower transition

region (LTR) to the corona. *TRACE* has not been able to provide adequate simultaneous observations because of technical limitations. The *TRACE* Lyα images suffer from significant levels of UV contamination, which makes their interpretation difficult especially when precise photometry is required (Handy et al. 1999b). We can now close this observational gap with Lyα observations from a new instrument, the Very High Angular Resolution Ultraviolet Telescope (VAULT; Korendyke et al. 2001). VAULT was flown as a sounding rocket payload on 1999 May 7 and acquired several Lyα images of an active region and the quiet Sun with subarcsecond ($\sim 0\farcs33$) resolution. *TRACE* supported the launch with a series of 171 Å images during the flight. In this paper, we investigate the relationship between the coronal and LTR structures using a pair of Lyα and 171 Å images. The two images were chosen because they have the largest spatial overlap among the available data and were obtained nearly simultaneously. A brief overview of the instruments and the data reduction is given in § 2. In § 3 we compare the structures seen in the two instruments, and in § 4 we discuss the results from our emission measure analysis and summarize our analysis.

1. INSTRUMENT DESCRIPTION AND OBSERVATIONS

VAULT consists of a 30 cm Cassegrain telescope followed by a zero-dispersion spectroheliograph (Bartoe & Brueckner 1978). It is designed to operate close to the Lyα Rayleigh diffraction limit ($\sim 0\farcs1$) with an angular resolution of $0\farcs33$ and a bandpass of 70 Å. The light is focused onto a lumogen-coated 3072×2048 CCD with a $0\farcs125$ pixel^{-1} pitch. The $257'' \times 386''$ field of view allows imaging of large-scale features (e.g., active regions, quiet Sun, etc.) with very high spatial resolution. The VAULT instrument is described in detail in Korendyke et al. (2001).

During the rocket flight, we obtained 16 full-field images with exposure times between 2 and 6 s. The field of view included part of NOAA active region 8525, a large filament, and quiet-Sun areas. The instrument achieved a resolution of $0\farcs33$ in the 2 s exposures. We use the best of these images here.

The VAULT images were corrected for bias and the dark current. The photometric calibration of the VAULT data was based on the assumption that the quiet-Sun Lyα flux does not vary significantly during the solar cycle and that it is uniformly distributed over the solar disk. Then, from the measured flux (in DN s^{-1}) in a quiet-Sun part of a VAULT image, we estimated the total Lyα flux at Earth. We derived a calibration factor by comparing the VAULT flux to the measurements of Prinz (1974), which have a photometric accuracy of $\lesssim 20\%$ (D. Prinz 2001, personal communication). We expect the same level of accuracy for the calibrated VAULT images. From the VAULT observations, for example, the predicted total Lyα flux at Earth on 1999 May 7 is $\sim 4.11 \times 10^{11}$ photons cm^{-2} s^{-1}. The Solar Ultraviolet Spectral Irradiance Monitor (SUSIM; Brueckner et al. 1993) measured 4.65×10^{11} photons cm^{-2} s^{-1} (data courtesy of L. Floyd), which is within the expected accuracy.

We processed the *TRACE* EUV images through the standard Solarsoft analysis routines. The *TRACE* 171 Å channel has a 6.4 Å passband and is actually centered at around 173 Å. The "171 Å" label is used to maintain consistency with the terminology of EIT. The 171 Å passband contains contributions from the Fe IX and Fe X lines and peaks at $\sim 9 \times 10^5$ K. Besides the EUV images, *TRACE* also provided context images in Lyα, 1500 Å, and 1600 Å before the rocket launch. The spatial resolution of the TRACE images is $\sim 1\farcs25$. We coregistered the *TRACE* and VAULT Lyα images, using common features, with an accuracy of a *TRACE* pixel ($\sim 0\farcs5$). This procedure also verified the VAULT plate scale and provided the solar coordinates of the VAULT pointing. Finally, the 171 Å images were co-aligned to the VAULT images by applying the most recently (as of 2001 February) known offsets between the 171 and Lyα *TRACE* channels. For the subsequent analysis, we chose the 19 s exposure 171 Å image taken at 20:02:41 UT and the 2 s exposure Lyα image taken at 20:02:44 UT.

2. RESULTS

The two images are shown in Figure 1. The boxes, marked R1 to R5, delineate certain representative areas that we consider in more detail later. The field of view contains mostly active region plage. The locations R1, R2, and R4 correspond to typical moss in the 171 Å image, as identified by their reticulated or mottled appearance, and R3 and R5 mark areas where EUV loops dominate. We have also examined the *Yohkoh*/SXT (Tsuneta et al. 1991) data taken in support of the VAULT launch. The SXT images show X-ray loops anchored in areas R1 and R2, as is expected in EUV moss areas (Berger et al. 1999), and in R3, although the moss is less visible in that area. Several loops overlie R4, but it is not clear if any of them are anchored there. No SXT loops exist over R5. Although several Lyα loops are visible in the VAULT image, the majority of the Lyα emission has a patchy appearance that is very similar to the *TRACE* moss. In fact, the overall resemblance is so close that one is tempted to conclude that the Lyα plage is the LTR footprint of the EUV moss. To test this hypothesis, we examine the correlation between the Lyα and EUV structures.

First, we examined the correlation between the VAULT and *TRACE* intensities. To reduce the confusion from unrelated structures, we traced regions of interest (ROIs) in each of the 171 Å boxes, avoiding low count areas, filaments, and large-scale loops. The intensities of the pixels within these ROIs are plotted in Figure 2. Also shown is the linear Pearson correlation coefficient. We see a very good correlation between the Lyα and 171 Å intensities in R1 and R4. The correlation diminishes greatly in the areas where the 171 Å loop emission is dominant (R3 and R5). At this stage, it is unclear if the lack of correlation is caused by the masking of the moss emission from the overlying loops (some moss can be seen through the EUV loops in R3, for example). We have verified that the correlation coefficients are statistically significant by calculating the probability that they arise from a random sample of uncorrelated data points (Bevington & Robinson 1992, eq. [11.18]). The probabilities were exceedingly small for all cases ($\ll 10^{-6}$), a result of the large number of data points ($N > 1000$) in each region. Because R1 has the smallest scatter, we used these points to look for a numerical fit between the two intensities, $I_{\mathrm{Ly}\alpha}$ and I_{171}. We found that the distribution of the data points can be described by a function of the form

$$I_{\mathrm{Ly}\alpha} = C_1[1 - C_2 \exp(-C_3 I_{171})] \ , \qquad (1)$$

where $C_1 = 1960$, $C_2 = 1.25$, and $C_3 = 0.21$. This function is plotted in all panels of Figure 2. It is apparent that the

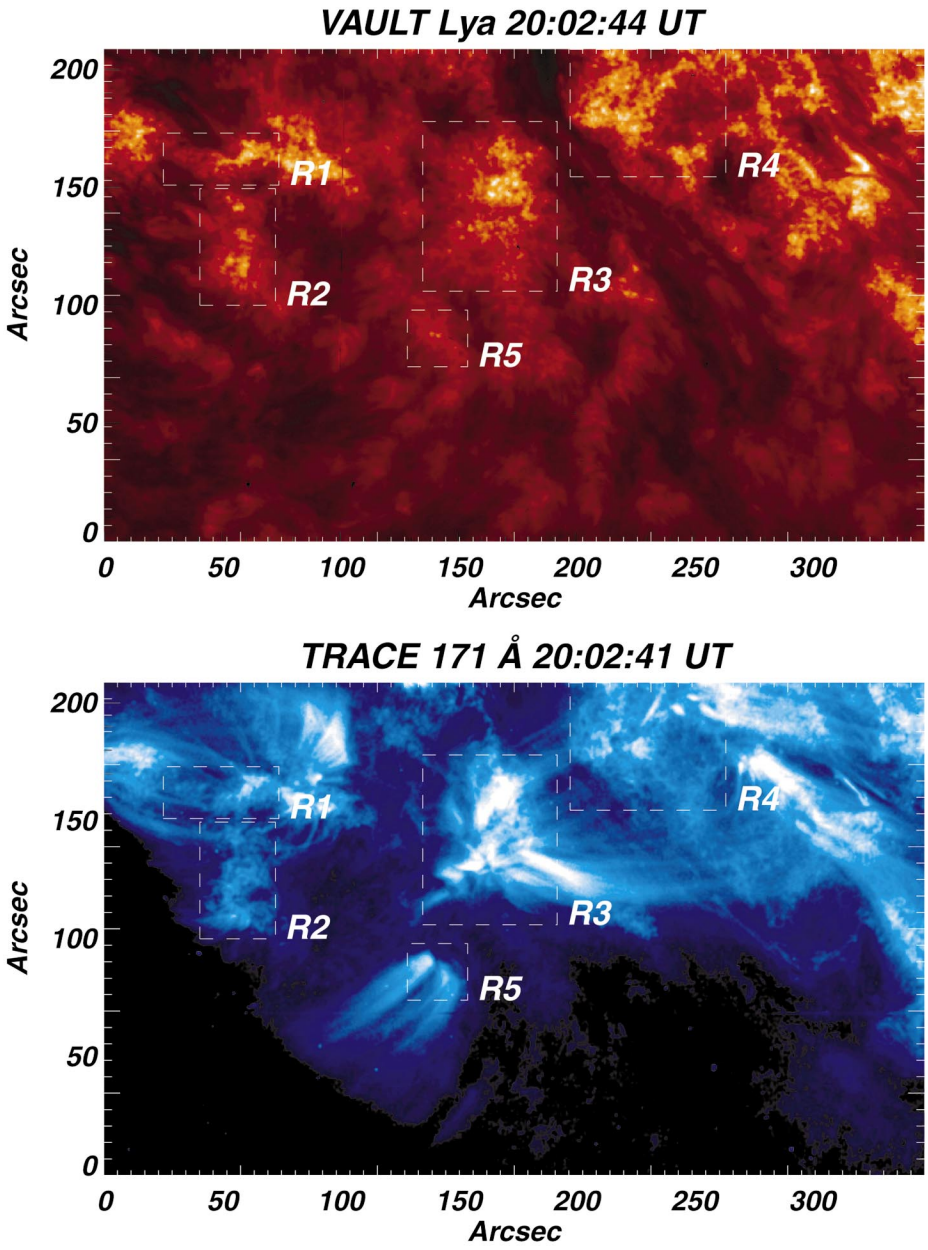

FIG. 1.—Part of active region 8525 in Lyα (*upper panel*) and 171 Å (*lower panel*). The instruments, wavelengths, and times for each image are shown on the plot. The center of the field of view is at N18°, W13°. The boxes mark those areas that were used for the analysis (see text).

function is also a good fit for R4 and for some of the points in R2. We reached similar conclusions for all plage areas that have strong moss morphology in the *TRACE* images. This result suggests that the mechanism responsible for the Lyα and 171 Å emissions is the same regardless of the moss intensity.

The scatter plots in Figure 2 give only a statistical sense for the correlation between the LTR and coronal emission but do not tell us much about the connectivity of individual structures. A careful visual inspection of the images reveals several areas where one can identify the same structures in the two wavelengths. A few examples from area R1 are marked by arrows in Figure 3. We see that moss structures in a range of scales (from about 1″ to 10″) appear highly similar in the two images. It is likely that the emissions arise from similar heights in the atmosphere, in agreement with past work (Berger et al. 1999). The close resemblance does not extend to the large scale EUV loops, however. The arrow labeled "5" in Figure 3 clearly shows a 171 Å emission loop that is in absorption in the VAULT image.

3. DISCUSSION

The observation that 171 Å and Lyα moss structures are so similar strongly suggests that they are physically linked. One obvious possibility is that they are magnetically connected and heated by a downward thermal conduction flux from the corona. We refer to this as the "standard model." In this interpretation, the 171 Å and Lyα emissions both originate in the transition region footpoints of hot ($T > 2$ MK) coronal loops. The 171 Å emission comes from the upper transition and thus a slightly greater height than the Lyα emission. Soft X-ray observations from *Yohkoh* reveal

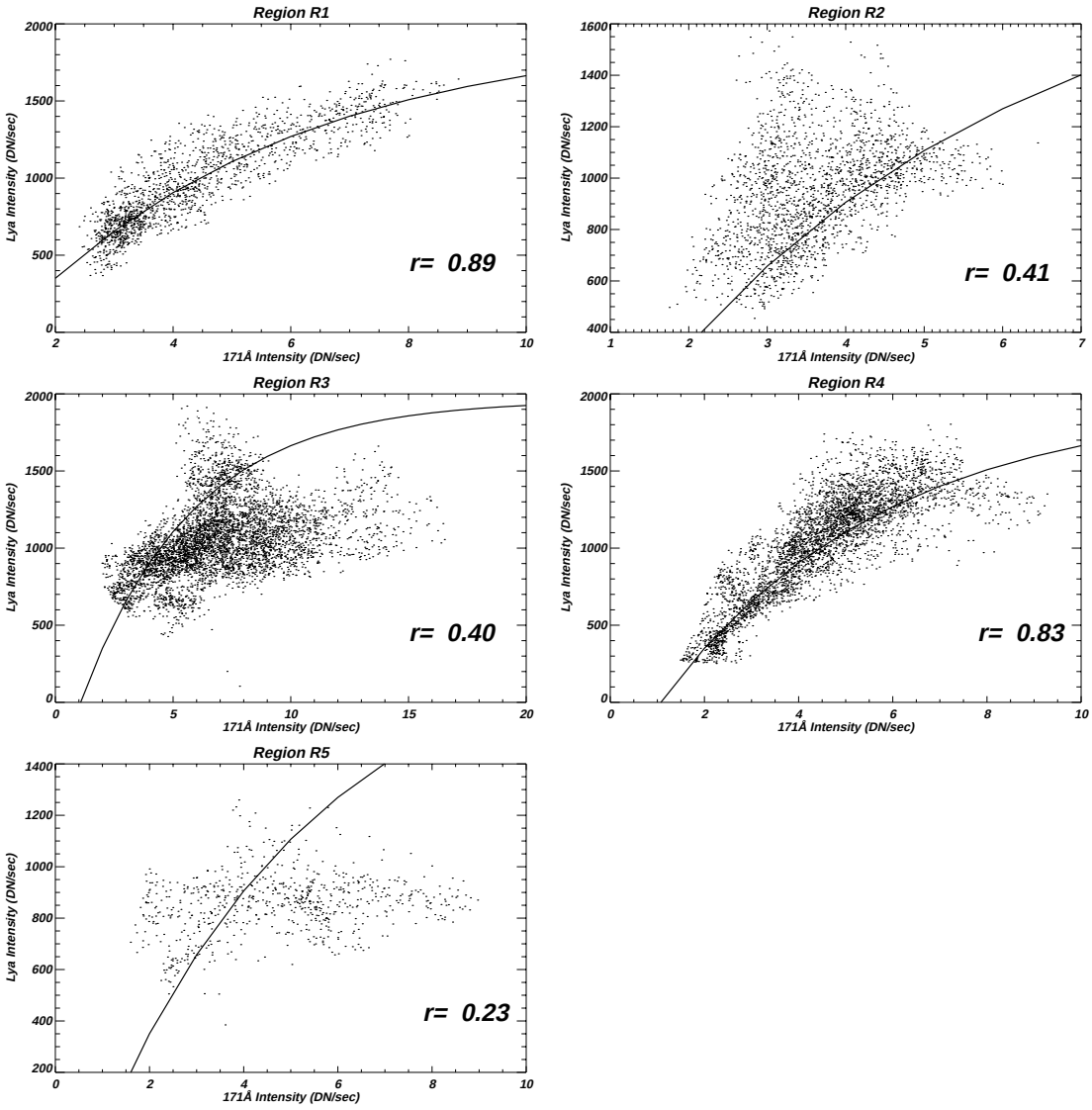

FIG. 2.—Scatter plots of the Lyα vs. the 171 Å intensity in subregions of the areas marked in Fig. 1. The linear Pearson correlation coefficient is also shown. The solid line is a fit to the points in region R1.

that multimillion-degree loops do indeed emanate from regions of 171 Å moss (Berger et al. 1999). Furthermore, the intensity of the moss is consistent with the intensity of the soft X-rays as predicted by the standard model (Martens, Kankelborg, & Berger 2000).

Lyα moss is also seen at the footpoints of "warm" ($T \sim 1$ MK) loops (e.g., regions R3 and R5 in Fig. 1). In these loops, the 171 Å emission comes from the long coronal section of the loop rather than the thin transition region footpoints. The basic picture that we infer from the observed morphology is indicated schematically in Figure 4, where we show logarithmic temperature profiles of hot and warm loops and indicate the locations of the Lyα and 171 Å emissions. Note that this picture explains quite naturally why Lyα moss has a greater spatial extent than does 171 Å moss. Lyα moss must occur wherever there is 171 Å moss, but it can also occur where 171 Å moss is missing (where the loops are warm). We can also understand why the spatial correlation between Lyα and 171 Å is diminished in regions of warm loops (regions R3 and R5 in Fig. 2): even if the coronal and transition region emissions vary together within each loop, a given line of sight will pass through the coronal (171 Å) sections of some loops and the footpoints (Lyα) of different loops.

If the standard model is correct, then we can predict theoretically how the Lyα and 171 Å intensities should be related and compare the predicted relationship with that seen in the observations. This is most easily done in regions of well-correlated moss (e.g., region R1), where both emissions are presumed to originate from the transition regions of hot loops. If the radiation is powered by a classical thermal conduction flux from the corona, F_c, then

$$n^2\Lambda(T) = -\frac{dF_c}{ds} \approx \frac{2}{7}\,\kappa_0\,\frac{T^{7/2}}{H(T)^2}\,, \qquad (2)$$

where s is the field line coordinate, n is the electron number density, κ_0 is the coefficient of thermal conductivity, $H(T) = (d\ln T/ds)^{-1}$ is the temperature scale length along the field, and $\Lambda(T)$ is the optically thin radiative loss function. We assume that Lyα is effectively optically thin, meaning that every collisional excitation results in a photon

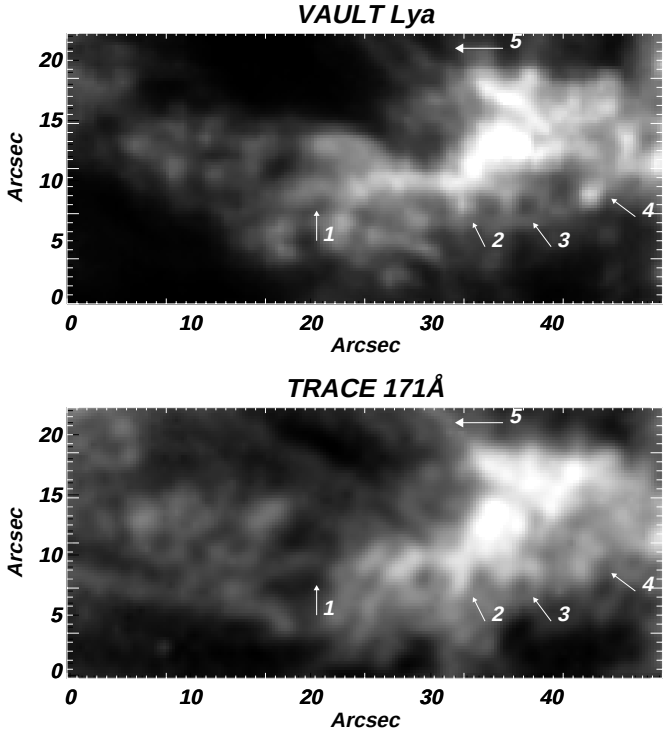

FIG. 3.—Region R1 in more detail. The arrows point to areas where similar structures can be seen in both wavelengths. Arrow 5 shows an 171 Å loop in absorption in the Lyα image.

that escapes the loop, perhaps after multiple scatterings (Athay 1986). This should be valid for most observed structures (Gouttebroze, Vial, & Tsiropoula 1986; Woods, Holzer, & MacGregor 1990). See McClymont & Canfield (1983) for a discussion of how $\Lambda(T)$ might be modified to account for optical depth effects. Solving equation (2) for $H(T)$ and substituting into the common definition of emission measure,

$$\mathrm{EM}(T) = n^2 H(T)\,, \tag{3}$$

we find that

$$\mathrm{EM}(T) \propto \Lambda(T)^{-1/2} T^{3/4} P\,, \tag{4}$$

where P is the total pressure. Since hydrogen is mostly ionized where Lyα is formed and above, we assume that $P \approx 2knT$, where k is Boltzmann's constant. In addition, if the height separation of Lyα and 171 Å is smaller than a gravitational scale height, we can assume they will be formed at approximately equal pressure within each loop. The ratio of the Lyα and 171 Å emission measures is then given by

$$\frac{\mathrm{EM}_{\mathrm{Ly}\alpha}}{\mathrm{EM}_{171}} \approx \left(\frac{\Lambda_{171}}{\Lambda_{\mathrm{Ly}\alpha}}\right)^{1/2} \left(\frac{T_{\mathrm{Ly}\alpha}}{T_{171}}\right)^{3/4} = 0.18\,, \tag{5}$$

where we take $T_{171} = 9 \times 10^5$ K, $T_{\mathrm{Ly}\alpha} = 2 \times 10^4$ K, $\Lambda_{\mathrm{Ly}\alpha} = 10^{-22}$ ergs cm^3 s^{-1}, and $\Lambda_{171} = 10^{-21}$ ergs cm^3 s^{-1} (e.g., Martens, Kankelborg, & Berger 2000, Fig. 3).

The observed *TRACE* intensities can be converted to emission measures by means of the 171 Å response function (Handy et al. 1999a). Following Martens, Kankelborg, & Berger (2000), we use the half-max of the response function, which gives 1 DN s^{-1} pixel^{-1} $\approx 1.8 \times 10^{26}$ cm^{-5}. To compute a contribution function for Lyα (the temperature dependence of the emissivity) we use the standard expression

$$\epsilon(T) = \frac{8.63 \times 10^{-6}}{4\pi T^{1/2}} \frac{\gamma}{g} e^{-\Delta E/kT} \frac{n_p}{n_{\mathrm{H}}}\,, \tag{6}$$

where g is the statistical weight of the lower level, γ is the effective collision strength (Scholz et al. 1990), T is the electron temperature, $\Delta E = 1.64 \times 10^{-11}$ ergs is the excitation energy, n_p is the proton number density, and n_{H} is the total hydrogen number density (protons plus neutrals). For the fractional ionization of hydrogen, n_p/n_{H}, we adopt the calculations of Mazzotta et al. (1998). The resulting contribution function is shown in Figure 5. Combining this with our photometric calibration of VAULT and assuming that the contribution function has an average value of 70% of its maximum over the line-forming region (e.g., Klimchuk & Cargill 2001), we find that 1 DN s^{-1} pixel^{-1} $\approx 1.1 \times 10^{26}$ cm^{-5}.

We applied these conversions to the observed intensities in region R1 and the results are shown in Figure 6. We see that the emission measure ratio is very different from that predicted by equation (5). The Lyα emission measure is about a factor of 100 larger than the 171 Å emission measure rather than a factor of 5 smaller. That is, based on the 171 Å intensities, Lyα is about 500 times brighter than expected from the standard model. This is a well-known problem. All observed emission cooler than about 2×10^5 K is brighter than predicted by the model, with the greatest discrepancy occurring at the coolest temperatures (e.g., Athay 1981; Feldman 1983; Mariska 1992).

There are several possible explanations for the excess brightness of Lyα. One idea is that the solar atmosphere is comprised of two distinct components—hot/warm loops (the standard model) and independent cool ($T < 2 \times 10^5$ K) structures. Presumably these other structures are cool loops with temperature profiles like that shown in Figure 4 (e.g.,

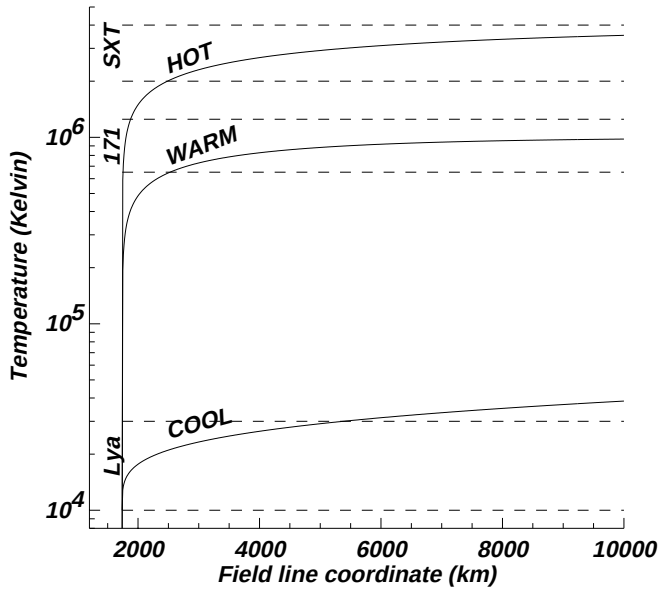

FIG. 4.—Typical temperature profiles for hot, "warm," and "cool" loops. The locations where emission in the Lyα, 171 Å, and SXT passbands originate are also marked.

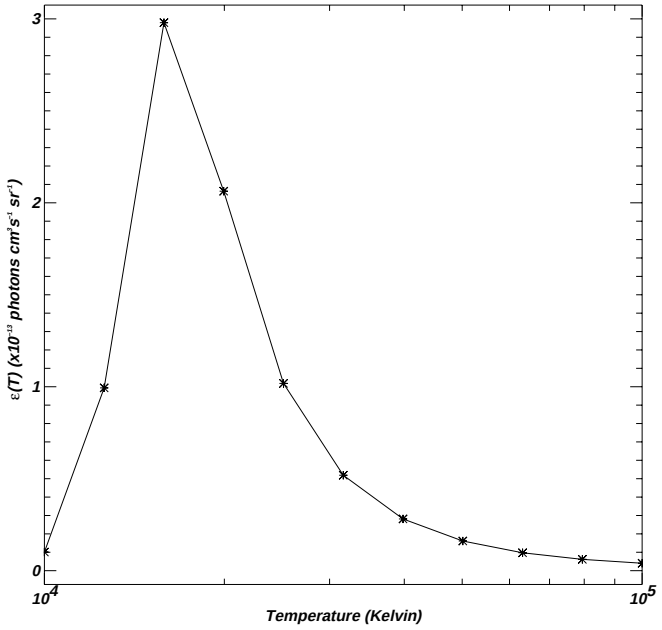

FIG. 5.—Lyα emissivity as calculated from eq. (6)

Antiochos & Noci 1986), but other possibilities have been proposed (Feldman 1994). A suitable mixture of hot/warm and cool loops might then explain the full temperature range of observed emission measures. In our opinion, the combined VAULT and *TRACE* data do not support this idea. The morphological similarities and detailed spatial correlation between the Lyα and 171 Å moss indicate that the two regimes are physically related. Furthermore, the appearance of the Lyα emission is not suggestive of short cool loops. This is not surprising, since moss is associated with active region plage areas, which tend to be unipolar. The possibility of short cool loops in the mixed polarity regions of the quiet Sun, however, is another matter.

If the Lyα and 171 Å features are indeed thermally linked along magnetic flux tubes, then how can the standard model be modified to explain the excess Lyα brightness? Among the possibilities are enhanced thermal conduction heating by tail electrons coming from higher in the transition region (Shoub 1983) and displacement of the Lyα contribution function toward higher temperatures, and hence higher excitation rates, by ambipolar diffusion of neutral hydrogen (Fontenla, Avrett, & Loeser 1991). Ionization nonequilibrium effects due to bulk mass motions may also be important (Raymond & Dupree 1978; Spadaro et al. 1990; Woods & Holzer 1991).

Perhaps the most straightforward explanation is enhanced mechanical heating in the lower transition region, especially where Lyα is formed (e.g., Jordan 1980; Woods, Holzer, & MacGregor 1990). In its original form, the standard model has transition region radiation being powered almost entirely by thermal conduction, but there is nothing to prevent direct mechanical heating from playing a dominant role in the lower layers (although see the discussion in Woods, Holzer, & MacGregor 1990 about the possibly unrealistic requirements on the form of the heating). If direct mechanical heating is indeed important, then based on the observed positive correlation between Lyα and 171 Å intensities, we can draw the interesting conclusion that the heating must itself be correlated between the lower transition and corona (recalling that the 171 Å moss in the upper transition region is heated primarily by thermal conduction from the corona and is therefore an indicator of coronal heating). Perhaps there is a single heating mechanism that operates in both regimes, or perhaps there are two different mechanisms that share a common dependence on, for example, the magnetic field strength. We will pursue this further in a later paper where we examine the correlation of Lyα and 171 Å with the observed photospheric field.

4. CONCLUSIONS AND SUMMARY

We have examined the small-scale morphological relationship between coronal and LTR emission over part of an active region using VAULT and *TRACE* images taken at a single time. We did not consider any evolutionary effects in the paper. Our analysis shows the following:

1. The EUV emission is always associated with Lyα emission but not the reverse. The Lyα and EUV emission arise from the same active region areas but the Lyα also extends to the quiet Sun. Both types of emission trace the chromospheric network.

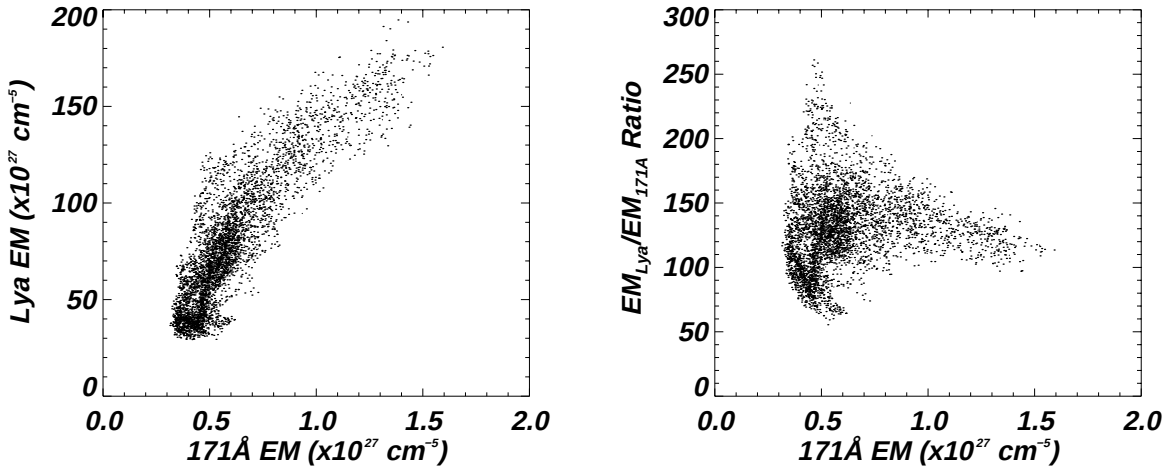

FIG. 6.—*Left panel*: Plot of the emission measures in region R1. *Right panel*: The ratio of the emission measures as a function of the 171 Å emission measure.

2. Lyα loops are visible in the quiet Sun but the emission takes a bright point character over the plage and looks very similar to the overlying *TRACE* moss.

3. The EUV and Lyα intensities correlate very well at the locations where *TRACE* moss emission is dominant. The scale sizes of the structures in the two regimes are also very similar. This implies that they originate at very similar heights. There is poor correlation at the footpoints of the *TRACE* loops. Also, the Lyα morphology is the same whether EUV loops or moss are present at that location.

4. In moss areas, we can trace several structures from the corona to the chromosphere/LTR. Not all *TRACE* sources, however, seem to have a LTR counterpart. This might be caused by obscuration from chromospheric jets (De Pontieu et al. 1999) or resolution effects, for example. Another possibility is the rearrangement of the magnetic field in the chromosphere as it was proposed by De Pontieu et al. (1999) for the case of the Ca K observations.

We conclude from these observations that the Lyα and 171 Å structures are physically linked. We suggest that the active region atmosphere is comprised of both hot ($T > 2$ MK) loops, which emit Lyα and 171 Å radiations from transition region footpoints, and warm ($T \sim 1$ MK) loops, which emit Lyα radiation from footpoints and 171 Å radiation from long coronal sections. The evidence argues against a cool ($T < 0.2$ MK) loop component. As found previously, the Lyα emission is much brighter than expected from the standard model in which the transition region is heated by a classical thermal conduction flux from the corona. If direct mechanical heating is responsible for the Lyα radiation, then this heating must be positively correlated with the heating of the corona above. This places a valuable constraint on the physical mechanism(s) of energy release.

We thank J. Cook, K. Dere, E. Landi, and D. T. Woods for many fruitful discussions and L. Floyd for providing the SUSIM Lyα data. The VAULT instrument development work has been supported by the Office of Naval Research task area SP033-02-43 and by NASA defense procurement request S-84002F. The work of J. A. K. was supported by the NASA SEC GI Program. T. D. T. and B. N. H. were supported by the *TRACE* contract at Lockheed Martin, NAS 5-38099.

REFERENCES

Antiochos, S. K., & Noci, G. 1986, ApJ, 301, 440
Athay, R. G. 1981, ApJ, 249, 340
———. 1986, ApJ, 308, 975
Bartoe, J.-D. F., & Brueckner, G. E. 1978, J. Opt. Soc. Am., 65, 13
Berger, T. E., de Pontieu, B., Schrijver, C. J., & Title, A. M. 1999, ApJ, 519, L97
Bevington, P. R., & Robinson, D. K. 1992, Data Reduction and Error Analysis for the Physical Sciences (2d ed.; Boston: WCB/McGraw-Hill)
Brueckner, G. E., Edlow, K. L., Floyd, L. E., Lean, J. L., & Vanhoosier, M. E. 1993, J. Geophys. Res., 98, 10695
Delaboudiniére, J.-P., et al. 1995, Sol. Phys., 162, 291
De Pontieu, B., Berger, T. E., Schrijver, C. J., & Title, A. M. 1999, Sol. Phys., 190, 419
Domingo, V., Fleck, B., & Poland, A. I. 1995, Sol. Phys., 162, 1
Feldman, U. 1983, ApJ, 275, 367
———. 1994, Phys. Plasmas, 1, 1390
Feldman, U., & Laming, J. M. 1994, ApJ, 434, 370
Fletcher, L., & De Pontieu, B. 1999, ApJ, 520, L135
Fontenla, J. M., Avrett, E. H., & Loeser, R. 1991, ApJ, 377, 712
Gabriel, A. H. 1976, Philos. Trans. R. Soc. London, A, 281, 339
Gouttebroze, P., Vial, J. C., & Tsiropoula, G. 1986, A&A, 154, 154
Handy, B. N., et al. 1999a, Sol. Phys., 187, 229
———. 1999b, Sol. Phys., 190, 351
Jordan, C. 1980, A&A, 86, 355
Klimchuk, J. A., & Cargill, P. J. 2001, ApJ, 553, 440
Korendyke, C. M., et al. 2001, Sol. Phys., 20, 63
———. 2001, Sol. Phys., in press
Mariska, J. T. 1992, The Solar Transition Region (Cambridge: Cambridge Univ. Press)
Martens, P. C. H., Kankelborg, C. C., & Berger, T. E. 2000, ApJ, 537, 471
Mazzotta, P., Mazzitelli, G., Colafrancesco, S., & Vittorio, N. 1998, A&AS, 133, 403
McClymont, A. N., & Canfield, R. A. 1983, ApJ, 265, 497
Peres, G., Reale, F., & Golub, L. 1994, ApJ, 422, 412
Prinz, D. K. 1974, ApJ, 187, 369
Raymond, J. C., & Dupree, A. K. 1978, ApJ, 222, 379
Scharmer, G. B., Brown, D. S., Peterson, L., & Reben, J. 1985, Appl. Opt., 24, 2558
Schrijver, C. J., et al. 1999, Sol. Phys., 187, 261
Scholz, T. T., Walters, H. R. J., Burke, P. G., & Scott, M. P. 1990, MNRAS, 242, 692
Shoub, E. C. 1983, ApJ, 266, 339
Spadaro, D., Zappala, R. A., Antiochos, S. K., Lanzafame, G., & Noci, G. 1990, ApJ, 362, 370
Tsuneta, S., et al. 1991, Sol. Phys., 136, 37
Wikstøl, Ø., Judge, P. G., & Hansteen, V. 1998, ApJ, 501, 895
Woods, D. T., & Holzer, T. E. 1991, ApJ, 375, 800
Woods, D. T., Holzer, T. E., & MacGregor, K. B. 1990, ApJ, 355, 295